

Deep upwelling and diffusivity in the southern Central Indian Basin

Mary C. McCarthy, Lynne D. Talley

Scripps Institution of Oceanography, La Jolla, CA

Molly O. Baringer

NOAA/Atlantic Oceanographic and Meteorological Laboratory, Miami, FL

Abstract. Transport of the deepest water westward through a gap at 28°S in the Ninetyeast Ridge between the Central Indian Basin and the West Australia Basin is calculated from hydrographic data collected as part of WOCE Hydrographic Program section I8N. Zero reference velocity levels at mid-depth were chosen through consideration of water masses. The small transport of 1.0 Sv westward of water denser than $\sigma_4 = 45.92 \text{ kg m}^{-3}$ through the gap must all upwell in the southern Central Indian Basin. Of this, 0.7 Sv upwells between the central and western sill sections, that is, close to the sill itself. Using the areas covered by the isopycnal, we calculate an average vertical velocity of $3.3 \cdot 10^{-3} \text{ cm s}^{-1}$ close to the sill and of $4.2 \cdot 10^{-4} \text{ cm s}^{-1}$ west of the sill. Associated average vertical diffusivities are $105 \text{ cm}^2 \text{ s}^{-1}$ close to the sill and $13 \text{ cm}^2 \text{ s}^{-1}$ west of the sill, in this bottom layer.

1. Introduction

The strength of upwelling and its associated diapycnal diffusivity has important implications for the heat budget and global climate, since it is the completing leg of the thermohaline circulation. Previous studies indicate that vertical diffusivities in the interior ocean are an order of magnitude lower than Munk's (1966) average vertical diffusivity of $1 \text{ cm}^2 \text{ s}^{-1}$ (Ledwell et al., 1993), which has led to the hypothesis that much larger rates of mixing occur near boundaries. Several recent groups of observations support this hypothesis (Hogg et al., 1982; Toole et al., 1994; Polzin et al., 1996; Roemmich et al., 1996). Special attention has been given to the Indian Ocean where Warren (1981), Stuver et al. (1983), and Toole and Warren (1993) found northward meridional transport of deep water into the Indian Ocean of 10 to 20 Sv below 2000 m, implying relatively large upwelling rates of $3 - 5 \cdot 10^{-5} \text{ cm s}^{-1}$. Fu (1983) suggests a weaker overturning than this, with much sparser data sets. Robbins and Toole (1997) also find a weaker overturning than Toole and Warren (1993) and an average diffusivity of $1-2 \text{ cm}^2 \text{ s}^{-1}$, in line with basin-averaged diffusivities dating back to Munk (1966). The possibility remains that rates in the Indian Ocean might be higher than those of the Pacific and Atlantic Oceans. Explanations for this possibility include the Indian Ocean's intricate bathymetry and/or its mon-

soonal forcing. Barton and Hill (1989) show an elevated diffusivity of $10 \text{ cm}^2 \text{ s}^{-1}$ below 4000 m for water flowing through the Amirante Trench into the Somali Basin; other estimates for deep passages are similarly high (Hogg et al., 1982; Roemmich et al., 1996; Polzin et al., 1996). Presumably an elevated overall deep diffusivity in the Indian Ocean could arise from it having a larger number of deep passages per unit area compared with other ocean basins.

Aside from providing a possible explanation for increased upwelling and diffusivity, the complex topography of the Indian Ocean creates a number of ideal locations for studying these rates. The Indian Ocean is comprised of three major basins separated by relatively shallow ridges which do not allow abyssal water to pass except through confined passages. Here we consider the Ninetyeast Ridge, which separates the Central Indian Basin from the West Australian Basin (Fig. 1). The principal deep passage is at 11°S (Warren, 1982; Mantyla and Reid, 1995). This overflow feeds a diffuse westward jet in the deep Central Indian Basin (Warren, *ibid*); the water fills a dome in the middle of the Basin on the meridional section at 80°E (Talley and Baringer, 1995, 1997). Very weak overflow was found at 5°S and no overflow at a possible passage at 2-3°S (Warren, 1982). Toole and Warren (1993) identified a weak overflow through a gap in the Ninetyeast Ridge at 28°S, where it meets the Broken Ridge, based on the few stations which they occupied in the southern Central Indian Basin. In this study, the abyssal flow across this southernmost sill, at 28°S, is investigated to determine westward transport, rate of upwelling in the southern Central Indian Basin, and average deep vertical diffusivity there.

2. Data

Our data come from the meridional Indian Ocean WHP section I8N at 80°E through the Central Indian Basin, angling to the 28°S sill. Three short sections were made in the vicinity of the sill: to the west, through the expected center, and to the east (Fig. 1). The commonly available digitized bathymetry suggested a relatively broad sill, with a maximum depth of 3400 m and a very broad, smooth slope on each side. The actual bathymetry along the cruise track (Fig. 2) was logged every 5 minutes from the ship's precision depth recorder (PDR). The measured bathymetry and the topography predicted from gravity (Smith and Sandwell, 1997) indicate a very narrow ($< 5 \text{ nm}$) fracture reaching 4400 m (Fig. 2) on the eastern section

Copyright 1997 by the American Geophysical Union.

Paper number 97GL02112.
0094-8534/97/97GL-02112\$05.00

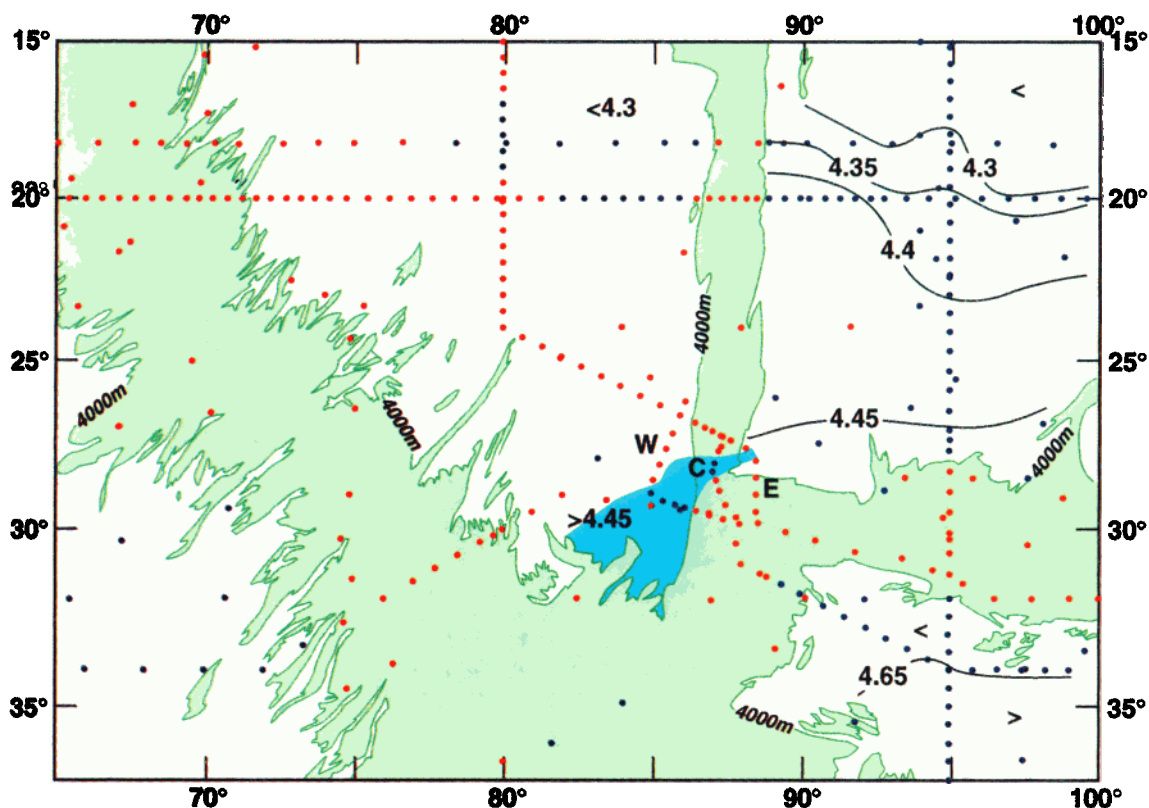


Figure 1. Hydrographic stations in the vicinity of the 28°S sill in the Ninetyeast Ridge with the 4000 m isobath based on the Gebco charts (green). Stations at 80°E looping to the sill are from the I8N cruise. Stations for the three meridional sill sections of Fig. 2 are indicated by W, C, and E. Stations at 95°E are from the WHP I9 cruise; at 20°S from the WHP I3 cruise, and along about 30°S from the 1987 cruise (Toole and Warren, 1993). Stations with waters denser than $\sigma_4 = 45.92 \text{ kg m}^{-3}$ are shown as blue dots, and stations with no water this dense as red dots. The blue shaded area is the nominal region of $\sigma_4 = 45.92 \text{ kg m}^{-3}$ water entering through the 28°S sill. Oxygen (ml l^{-1}) at $\sigma_4 = 45.92 \text{ kg m}^{-3}$ is contoured at 0.05 ml l^{-1} ; all values in the Central Indian Basin are 4.45–4.5 (south) or 4.25–4.3 (central).

and a deeper than expected fracture zone type structure through the center and on the western section.

Temperature, salinity, and pressure were measured with a CTD. A 36-bottle rosette sampler was used for salinity and oxygen calibration samples and for nutrients and other tracers (Talley and Baringer, 1995, 1997). Complete details concerning data collection and processing are available from the cruise report at the WOCE Hydrographic Programme Office.

Direct velocity observations were taken using accurate GPS navigation data and two acoustic Doppler current profiler (ADCP) systems, the hull-mounted ADCP and a lowered ADCP (LADCP) mounted on the rosette with the CTD. Unfortunately, in the region of our interest, around the 28°S sill, the lack of reflectors in the deep ocean resulted in a significantly degraded signal, so these profiles were not used for our study. (However, rough LADCP velocity sections do not contradict the choice of velocity reference levels described below.)

3. Transport, upwelling and diffusivity estimates

Our calculation consists of three steps, beginning with choosing the thickest bottom layer possible which feeds an isolated region in the Central Indian Basin un-

contaminated by other deep sources. After computing the transport into this layer through the 28°S sill, the upwelling velocity out of its upper surface can be computed. Finally, using the average vertical stratification at the top of the layer we arrive at the rate of diffusivity.

Examination of deep properties in the Central Basin suggests that most water deeper than about 3200 m enters from the sills in the Ninetyeast Ridge. Slightly shallower waters (circumpolar water) can also enter directly from the south (e.g. Toole and Warren, 1993). Here we consider water in an isolated deep layer whose only source can be the Ninetyeast Ridge at 28°S. This deeper layer is bounded by the $\sigma_4 = 45.92 \text{ kg m}^{-3}$ isopycnal (about 4000 m) based on historical hydrographic data, the 1987 32°S section, and the new WOCE hydrographic data (Fig. 1). Water this dense entering the Central Basin through the 11°S sill is separated spatially from the 28°S water and has markedly lower oxygen (Fig. 1). Since no stations shallower than 4000 m have water this dense, the 4000 m isobath was chosen as the southeastern boundary of the region. The area enclosed by these boundaries (91900 km^2) represents an upper bound on the area of the $\sigma_4 = 45.92 \text{ kg m}^{-3}$ isopycnal (blue shading in Fig. 1).

The western section (stations 377–386) and central section (stations 387–393) were used for transport calculations. The fracture zone was narrower than ex-

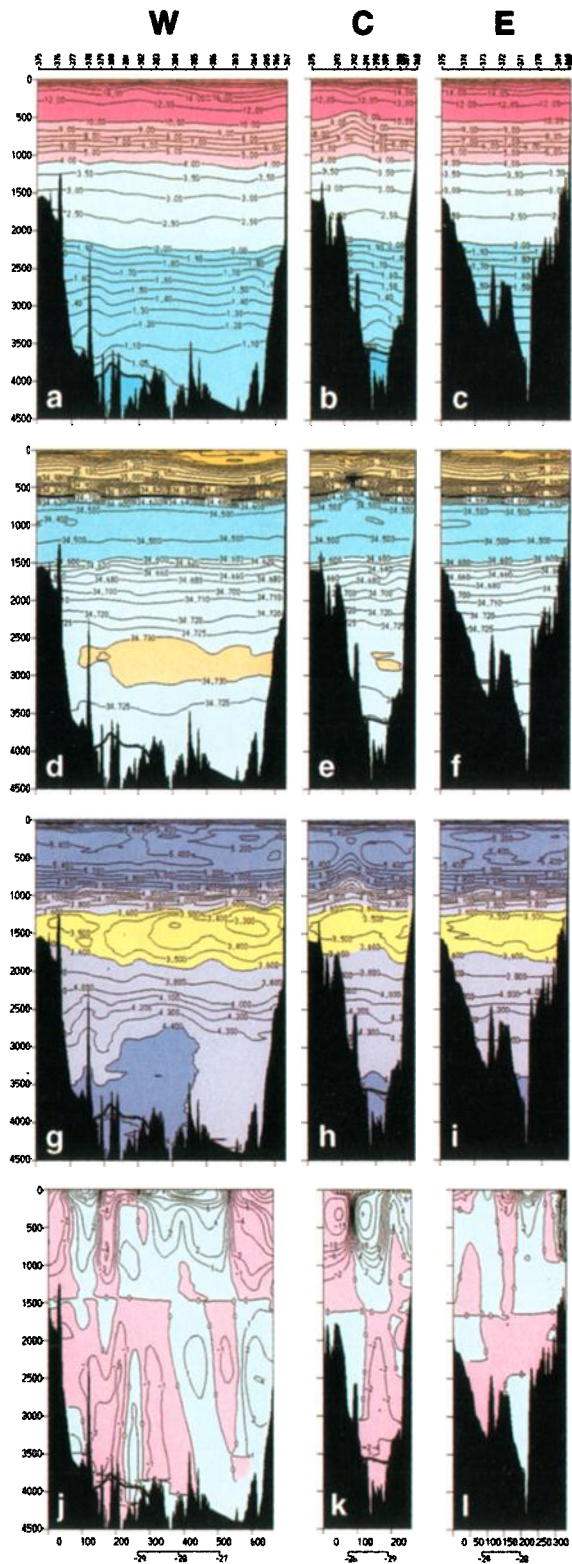


Figure 2. (a-c) Potential temperature ($^{\circ}\text{C}$) at the western (W), central (C), and eastern (E) sill sections. (d-f) Salinity at the same. (g-i) Oxygen (ml/l) at the same. (j) Geostrophic velocity at the western section relative to zero velocity at $\sigma_2 = 36.7 \text{ kg m}^{-3}$. (k-l) Geostrophic velocity at the central and eastern sections relative to zero velocity at $\sigma_2 = 36.8 \text{ kg m}^{-3}$. On the western and central sections, the $\sigma_4 = 45.92 \text{ kg m}^{-3}$ contour is overlain. Section locations are shown in Fig. 1.

pected on the eastern section, and no abyssal water was sampled there. Reference levels were chosen using distributions of salinity and oxygen (Fig. 2). For their zonal sections, Warren (1981) and Toole and Warren (1993) initially chose zero velocity levels near the oxygen minimum layer and adjusted them locally based on water properties. There is no a priori reason for a similar choice of reference level for our short, predominantly meridional sections over very complex topography. However, examination of water properties and geostrophic shear from the new WHP sections suggests that even here the oxygen minimum layer is a reasonable initial choice for zero velocity. Large-scale property distributions indicate that the high density, low temperature, high oxygen bottom water must be flowing west on average, with deep eastward flow on the northern side of the gap (low oxygen and high salinity). The low oxygen in the oxygen minimum on the north side of the gap on the western section penetrates weakly into the central section and not at all into the eastern section (Fig. 2), suggesting very weak eastward flow at this level. Therefore we have chosen zero velocity at $\sigma_2 = 36.7 \text{ kg m}^{-3}$ (about 1450 m) on the western section, and zero velocity at $\sigma_2 = 36.8 \text{ kg m}^{-3}$ (about 1650 m) on the central and eastern sections to produce the circulation implied by large-scale property distribution.

The western geostrophic velocity section (Fig. 2j) shows eastward flow in the top and center, and westward flow on the sides. For the central section, the geostrophic velocities (Fig. 2k) are eastward to about 2000 m in the north, and westward below. In the south, flow is westward except at the very bottom.

Transports are sensitive to both reference level selection and the method for extrapolating velocity below the deepest common depth of each station pair. Our primary approach for the latter was to use a constant shear to the bottom. Error bounds for transports were estimated by comparison with results from other extrapolation methods and other reasonable reference level choices (for example, using zero velocity along $\sigma_2 = 36.5 \text{ kg m}^{-3}$ [about 1150 m] to 36.9 kg m^{-3} [about 2000 m] isopycnals). Reference levels had by far the greatest impact on transports.

Transport below $\sigma_4 = 45.92 \text{ kg m}^{-3}$ through the center section (stations 388 to 391) relative to $\sigma_2 = 36.8 \text{ kg m}^{-3}$ is 1.0 Sv westward. The range is $\pm 0.4 \text{ Sv}$ based on reference levels and $\pm 0.2 \text{ Sv}$ based on various extrapolation methods. Transport through the western section (stations 377-386) was significantly lower: 0.3 Sv westward $\pm 0.1 \text{ Sv}$.

The central section transport estimate and the isolated isopycnal area in the Central Indian Basin (Fig. 1) result in an average upwelling rate across $\sigma_4 = 45.92 \text{ kg m}^{-3}$ of $1.1 \cdot 10^{-3} \text{ cm s}^{-1}$. Applying the formula,

$$\kappa = \frac{T(\rho_{45.92}) - \iint u\rho dA}{A_{45.92} \partial\rho/\partial z}$$

yields a vertical diffusivity of $35 \pm 14 \text{ cm}^2 \text{ s}^{-1}$, where T is the transport upward across $\sigma_4 = 45.92 \text{ kg m}^{-3}$, the integral is over the flow of water denser than this through the gap, A is the area of the $\sigma_4 = 45.92 \text{ kg m}^{-3}$ isopycnal west of the gap, and $\partial\rho/\partial z$ is the average vertical density gradient at $\sigma_4 = 45.92 \text{ kg m}^{-3}$ calculated from I8N stations and 32 $^{\circ}\text{S}$ stations in this

small region. The error of $\pm 14 \text{ cm}^2 \text{ s}^{-1}$ results from the 0.4 Sv "error" in transport.

The difference in transport between the western and central sections is consistent with upwelling between them. The area between the two sections at $\sigma_4 = 45.92 \text{ kg m}^{-3}$ is about 21200 km^2 . The difference in transport between them is 0.7 Sv. The upwelling velocity thereby calculated is $3.3 \cdot 10^{-3} \text{ cm s}^{-1}$, and the diffusivity is $105 \text{ cm}^2 \text{ s}^{-1}$. Using just the transport through the western section and the isopycnal region to its west, which therefore characterizes a region outside the narrow sill, the upwelling is $4.2 \cdot 10^{-4} \text{ cm s}^{-1}$, and the diffusivity is $13 \text{ cm}^2 \text{ s}^{-1}$ for this bottom layer.

4. Summary and Concluding Remarks

Our estimated diffusivities fall within the range of values estimated for near-bottom layers in the Atlantic and Pacific Oceans. Our bottom layer depth ranges from 0 to about 400 m in the 28°S gap. Directly comparable estimates are: Hogg et al.'s (1982) estimates for the Vema Channel in the Brazil Basin, of $\kappa = 3.4 - 4.0 \text{ cm}^2 \text{ s}^{-1}$ for the bottommost layer of several hundred meters thickness; Barton and Hill's (1989) estimate of $10 \text{ cm}^2 \text{ s}^{-1}$ below 4000 m for the Amirante Trench; Polzin et al.'s (1996) estimate of $150 \text{ cm}^2 \text{ s}^{-1}$ at the bottom in the Romanche Fracture Zone in the Atlantic; and Roemmich et al.'s (1996) estimates for more finely subdivided near-bottom layers in the Samoan Passage in the South Pacific of $50\text{-}500 \text{ cm}^2 \text{ s}^{-1}$ for the bottommost layer of about 400 m thickness to $1 \text{ cm}^2 \text{ s}^{-1}$ for the layer 900 meters above the bottom. These diffusivities and the ones we calculate are clearly larger than the interior ocean diffusivities of order 0.1 to $0.5 \text{ cm}^2 \text{ s}^{-1}$ found by Ledwell et al. (1993) in the subtropical Atlantic and by Toole et al. (1994) in the northeast Atlantic and northeast Pacific, and average near-surface values on the order of $1 \text{ cm}^2 \text{ s}^{-1}$, decreasing with increasing depth, found by Zhang and Talley (1997).

While the 28°S sill may be insignificant for the large-scale transports in the Indian Ocean, this upwelling and diffusivity estimate confirms similarly high deep upwelling and diffusivities, and suggests that the values are much higher within the sill than in the still near-bottom layer away from the sill. A much more complete treatment of the data from this sill will include evaluation of fine structure, layer depths and stratification. Similar calculations will be made for many other deep gaps in the Indian Ocean. It remains to be seen if the Indian Ocean actually has larger deep diffusivity overall than the Atlantic or Pacific Oceans.

Acknowledgments. The collection of this WOCE data was funded by the National Science Foundation Ocean Sciences grant OCE-9413160. Data were collected and processed by the Scripps Oceanographic Institution's Oceanographic Data Facility. We thank the captain and crew of the R/V Knorr for their support. J. Hummon and E. Firing provided LADCP data and much advice about their use and potential misuse. The WOCE data in Fig. 2 along 95°E and 20°S were collected and furnished by A. Gordon, M. McCartney, B. Warren and W. Nowlin. MCM was funded by a National Defense Science and Engineering Graduate fellowship.

References

- Barton, E. D. and A. E. Hill, Abyssal flow through the Amirante Trench (western Indian Ocean), *Deep-Sea Res.*, **36**, 1121-1126, 1989.
- Fu, L.-L., Mass, heat and freshwater fluxes in the South Indian Ocean, *J. Phys. Oceanogr.*, **16**, 1683-1693, 1983.
- Hogg, N., P. Biscaye, W. Gardner and W. J. Schmitz Jr., On the transport and modification of Antarctic Bottom Water in the Vema Channel, *J. Mar. Res.*, **40S**, 231-263, 1982.
- Ledwell, J.R., A. J. Watson and C. S. Law, Evidence for slow mixing across the pycnocline from an open-ocean tracer-release experiment, *Nature*, **364**, 701-703, 1993.
- Mantyla, A. W. and J. L. Reid, On the origins of deep and bottom waters of the Indian Ocean, *J. Geophys. Res.*, **100**, 2417-2439, 1995.
- Munk, W. H., Abyssal recipes, *Deep-Sea Res.*, **13**, 707-730, 1966.
- Polzin, K. L., K. G. Speer, J. M. Toole, and R. W. Schmitt, Intense mixing of Antarctic Bottom Water in the equatorial Atlantic Ocean, *Nature*, **380**, 54-57, 1996.
- Robbins, P. E. and J. M. Toole, The dissolved silica budget as a constraint on the meridional overturning circulation of the Indian Ocean, *Deep-Sea Res.*, in press, 1997.
- Roemmich, D., S. Hautala and D. Rudnick, Northward abyssal transport through the Samoan passage and adjacent regions, *J. Geophys. Res.*, **101**, 14039-14055, 1996.
- Smith, W. H. F. and D. T. Sandwell, Global seafloor topography from satellite altimetry and ship depth soundings, submitted to *Science*, April 7, 1997.
- Stuiver, M., P. D. Quay and H. G. Ostlund, Abyssal water carbon-14 distribution and the age of the world oceans, *Science*, **219**, 849-851, 1983.
- Talley, L. D. and M. O. Baringer, Preliminary results from a WHP section in the Central Indian Ocean, *Int. WOCE Newsletter*, **21**, 35-38, 1995.
- Talley, L. D. and M. O. Baringer, Preliminary results from WOCE hydrographic sections at 80°E and 32°S in the Central Indian Ocean, *Geophys. Res. Lett.*, this issue, 1997.
- Toole, J. M. and B.A. Warren, A hydrographic section across the subtropical South Indian Ocean, *Deep-Sea Res.*, **40**, 1973-2019, 1993.
- Toole, J. M., K. L. Polzin, and R. W. Schmitt, Estimates of diapycnal mixing in the abyssal ocean, *Science*, **264**, 1120-1123, 1994.
- Warren, B. A., Transindian hydrographic section at lat. 18°S : Property distributions and circulation in the South Indian Ocean, *Deep-Sea Res.*, **28**, 759-788, 1981.
- Warren, B. A., The deep water of the Central Indian Basin, *J. Mar. Res.*, **40S**, 823-860, 1982.
- Zhang, H.-M. and L. D. Talley, Heat and buoyancy budgets and mixing rates in the upper thermocline, Submitted to *J. Phys. Oceanogr.*, 1997.

Mary C. McCarthy and Lynne D. Talley, Scripps Institution of Oceanography, La Jolla, CA 92093-0230 USA (e-mail: mcmccart@ucsd.edu and ltalley@ucsd.edu)

Molly O. Baringer, NOAA/AOML, Miami, FL 33149 USA (e-mail: baringer@aoml.noaa.gov)

(Received April 2, 1997; revised June 19, 1997; accepted July 8, 1997.)